Evaluation Of Subsurface Competence Using Shear-Wave Velocity and Geotechnical Indices from MASW Data in FCE(T) Akoka Campus, Lagos.

Babatunde, P and Ajayi, A. A. (Ph.D.)

Department of Physics Education

Federal College of Education (Technical), Akoka

peterfraayo77@gmail.com;

Abstract

The increasing incidence of structural defects such as wall cracks, tilting, settlement, and sinking of buildings within Federal College of Education (Technical), Akoka Campus, Lagos, necessitated an assessment of subsurface competence for safe construction. Seven MASW profiles were acquired along six traverses using a 24-channel ABEM seismograph, A 6kg sledgehammer and a metallic strike plate as the seismic source. Data acquisition involved 9-11 shot points per profile with multiple stacking to enhance signal quality. The acquired data were processed using Seisimager/SW software to obtain shear wave velocity (Vs) models and geotechnical parameters were derived to evaluate soil competence. The results revealed three subsurface layers across the profiles comprising silty clay, clay, sandy clay/clayey sand, sand/gravelly sand and firm soil. Vs values ranged from 97 m/s to 1042 m/s. Computed geotechnical indices showed low concentration index values (3.01-3.34), low material index values (-0.98 - -0.70) and stress ratio values ranging from 0.74 to 0.99 indicating predominantly incompetent to slightly competent near surface materials while more competent layers occurred at deeper horizons. The study recommends proper ground improvement measures prior to heavy construction activities to ensure long-term stability and safety.

Keywords: MASW, Shear Wave Velocity, Subsurface Competence, Geotechnical indices

Introduction

Multichannel Analysis of Surface Waves (MASW) was conducted along seven profiles within six traverses (TR1-TR6) were to map and characterize the subsurface layers beneath the Federal College of Education (Technical) Akoka Community, Yaba, Lagos state, South-Western Nigeria. The study area lies between Longitude 3º 22' 55" E and 3º 23' 5.3″ E. Latitude 06º 31'10" N and 06º 31'30" N.

This study was undertaken as a preliminary investigation into causes of structural defects observed in buildings within the study area. These defects include wall cracks, tilting and foundation settlement, which have contributed to building failures and have resulted in some structures being marked for demolition and evacuation by relevant government authorities.

Shortage of accommodation facilities, including lecture rooms, staff offices, staff quarters and student hostels has been a major concern for the College management. This challenge has been exacerbated by the fact that some existing structures are distressed, abandoned, or earmarked for demolition. Consequently, there is a need to provide safe, reliable, durable, and habitable buildings that will guarantee the safety of lives and property while promoting a conducive teaching and learning environment.

In seismic investigation, seismic waves are generated by a controlled source and propagate through the subsurface before returning to the surface through reflection, refraction, or propagation or travelling along subsurface interfaces. Geophones linearly positioned along the ground surface are used to record the travel times of these waves at varying distances from the source (Kearey et al. 2002). These travel times are subsequently converted into depth information, enabling the mapping of subsurface geological boundaries. Seismic waves are broadly divided into two categories; body waves and surface waves. Body waves travel through the earth's interior and consist of compressional (P-waves) and shear (S-waves). Surface waves travel along the interfaces between different media and are the result from the interference of P-waves and S-waves (Xia et al. 2002). A non-invasive seismic technique called the Multichannel Analysis of Surface Waves (MASW) was developed to determine the multilayered subsurface stratigraphy using the dispersive properties of surface waves. Approximately 70% of the seismic energy generated at the ground surface propagates as a surface waves. The MASW technique uses Rayleigh waves to estimate the near surface elastic properties of the subsurface (Park et al. 1999). The MASW technique has been successfully applied in pavement characterization, void detection (Park et al. 1999 and seabed sediment investigations. Dispersion occurs because waves of different frequency, wavelength, and phase velocities travel through heterogenous subsurface materials (Foti et al.

2003). When more than one phase velocity exists at a particular frequency, the phenomenon is called multimodal dispersion. The slowest phase velocity corresponds to the fundamental mode while higher phase velocities correspond to higher order modes (Taipodia et al. 2015).

Some limitations associated seismic refraction methods, such as hidden layer, velocity inversions, blind zone can be overcome using surface wave techniques (Foti et al. 2003). However, a noticeable limitation of the surface-wave technique is its trade-off between lateral resolution and depth of investigation. The effective depth of penetration of a surface wave theoretically is commonly taken as one wavelength, with most of the energy concentrated between the surface and depth of one-third of the maximum resolved wavelength (Park et al. 1999). High frequency (short wavelength) waves primarily sampled shallow subsurface layers whereas low frequency (long wavelength) waves penetrate deeper into the ground. (Lai and Wilmanski 2005).

The phase difference as a function of frequency between two adjacent geophone is estimated using equation (1)

$$\Delta\phi(f) = phase[G(f)F^*(f)]\Delta\phi(f) = phase[G(f)F^*(f)] \quad \ldots\ldots\ldots\ldots\ldots \quad (1)$$

where: G(f) and F(f) are the Fourier transforms of the time signals from the second and first receivers respectively and (*) represents the complex conjugate. The phase velocity at a given frequency (f) with spacing between adjacent geophones (Δx) is given by Eq. 2.

$$V_{phase}(f) = 2\pi f \frac{\Delta x}{\Delta\phi(f)} V_{phase}(f) = 2\pi f \frac{\Delta x}{\Delta\phi(f)} \quad \ldots\ldots\ldots\ldots \quad (2)$$

Using the half-wavelength condition, Rix and Leipski (1991) proposed that the maximum depth of penetration (Z_{max}) for which Vs can be reasonably estimated to be equal to about half the longest wavelength (λ_{max}) measured and it is given in Eq. 3.

$$Z_{\max} = \frac{\lambda_{\max}}{2} = 0.5\frac{V_{phase_{\min}}}{f_{\min}} \quad \ldots\ldots\ldots\ldots\ldots\ldots\ldots \quad (3)$$

Also, the thickness Hi of the uppermost layer limiting the resolution of subsurface is given in Eq.4

$$H_i \geq 0.5\lambda_{\min} = 0.5\frac{V_{phase\min}}{f_{\min}} \quad \ldots\ldots\ldots\ldots\ldots\ldots\ldots \quad (4)$$

where: $V_{phase\ max}$ and $V_{phase\ min}$are the maximum and minimum phase velocities of the fundamental mode respectively. f_{min} and f_{max} are corresponding minimum and maximum frequencies at phase velocity measured. The maximum wavelength (λmax) is related to the maximum spread length or array length (L), whereas the minimum wavelength (λmin) is related to the minimum distance (2dx) between geophones (O'Neill 2003 in Ezersky et al., 2013). Shortage of building accommodations in the form of lecture rooms, lecturers' offices, staff quarters and hostels for both students and their lecturers has been a concerned for the College management since some of the available ones are distressed, abandoned and marked for demolition. This study was necessary because of the need to provide good working environment, reliable and habitable housing accommodation that will last long, give no complain and guarantee safety of life and properties of both staff and students in the form of classrooms, offices, staff quarters and hostels is of utmost priority toward ensuring conducive teaching and learning environment.

Materials and Methods

Study Area

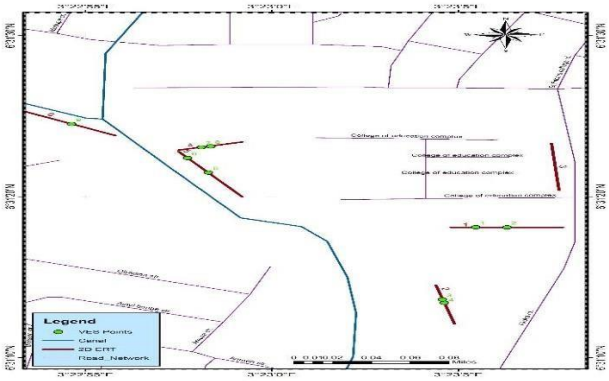

Figure 1: Base map of the study area

The study area (Figure 1) is Federal College of Education (Tech), Akoka, Yaba, Lagos State which falls within Lagos Mainland Local Government Area of Lagos State. Lagos State is one of the

Nigerian states bounded in the north by Ogun State, south by Atlantic Ocean and west by Benin Republic. The study area is located in sub-equatorial (South) climate which is characterised with heavy rainfall with two periods of maximum rainfall (that is June/July and September/October), convectional type of rainfall, all months of the year rainfall, low annual range of temperature, high relative humidity and long period of rainfall (8-10 months). There are two distinct seasons in the state, namely, the rainy season which lasts from March/April to October/November and the dry season which lasts for the rest of the year. Lagos State is a zone of coastal Creeks and Lagoons (Pugh 1954) developed by barrier beaches associated with sand deposits (Hill and Webb 1958 in Ajayi et al, 2023). The land topography is relatively flat and the surface geology is sedimentary characterised by complex geologies of alternating sequences of clay and sand deposits (ranging from silt, clay, and fine to coarse grained sand) forming the youngest stratigraphy called Benin Formation (Miocene to Recent) and Recent littoral alluvial deposits. The Benin Formation consists majorly of yellowish (Ferruginous) and white sand bodies (Jones & Hockey, 1964). The geomorphologic sub-units recognised in the area are Abeokuta, Imo group (Ewekoro and Akinbo), Oshoshun/Ilaro and Benin Formations (Adegoke et al., 2010). All these formations fall within the Dahomey Basin believed to be formed during the commencement of rifting, associated with the opening of the Gulf of Guinea in the early Cretaceous to late Jurassic (Adegoke et al. 2010). The Dahomey Basin extends from the south eastern Ghana through Togo and Benin Republic on the West side to the Okitipupa ridge/Benin Hinge line in the east side in the southern part of Nigeria (Adegoke et al., 2010). The geology of the basin had been improved through the availability of boreholes and recent road cuts. A simplified geological map of the study area is shown in figure 2.

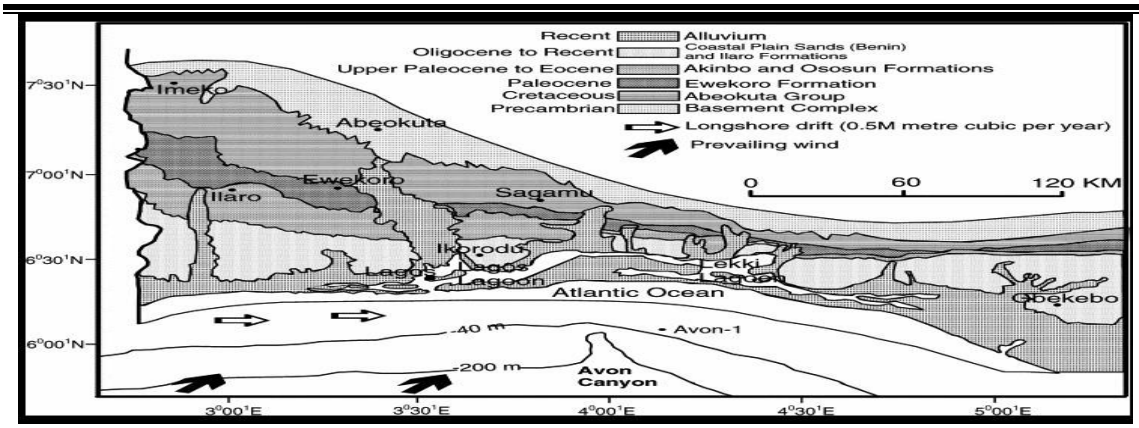

Figure 2: Geological map of LagosMethodology

The seismic waves were recorded using a 24-channel ABEM seismograph, powered by a 12-volt battery, a 6-kg sledgehammer and a metallic plate were used to generate seismic waves, with a sampling interval of 0.250ms and a total record length of 512 ms. Each seismic line was subjected to 9 –11 shot points, with 3-5 stacking applied at each shot point to reduce background noise and improve the signal-to-noise ratio. In order to achieve adequate ray coverage through the medium, two to three off-set shots were taken at distances of 2m to 6m from the first and last geophones. The remaining shots were taken at intervals of 2m to 5m in between the spread length. The description of various shot points and number of profiles acquired for the acquisition are summarized in the Table 1.

Table 1: Description of various shot locations with number of profiles acquired.

Location	Latitude (in degree)	Longitude (in degree)	Geophone intervals (m)	Shot location (m)	No. of profiles
1	3° 23’ 7.8 E	6° 31’ 23.2” N	3	-4, -2, 4.5, 16.5, 34.6, 52.5, 64.5, 71, 73, 75	1
2	3° 23’ 4.6 E	6° 31’ 19.3 N	3	-6, -4, -2, 4.5, 16.5, 34.6, 52.5, 64.5, 71, 73, 75	1
3	3° 23’ 6.2 E	6° 31’ 18.0 N	2	-4, -2, 3, 11, 23, 35, 43, 48, 50	2
4	3° 22’ 57.7 E	6° 31’ 22.9 N	2	-6, 4, -2, 3, 11, 23, 35, 43, 48, 50	1
5	3° 23’ 57.2 E	6° 31’ 57.2 N	3	-6, -4, -2, 4.5, 16.5, 34.6, 52.5, 64.5, 71, 73, 75	1
6	3° 23’ 53.6 E	6° 31’ 25.1 N	5	-10. -5, 7.5, 27.5, 57.5, 87.5, 107.5, 120, 125	1
7	3° 23’ 55.10 E	6° 31’ 24.1 N	3	-6, -4, -2, 4.5, 16.5, 34.6, 52.5, 64.5, 71, 73,	1

The acquired MASW data were processed and interpreted using Seisimager/SW software to determine shear wave velocity (Vs). The seismic raw data were processed and analysed using the Seisimager/SW Software. The procedure of MASW consists of four steps as shown in Figures 3 and 4.

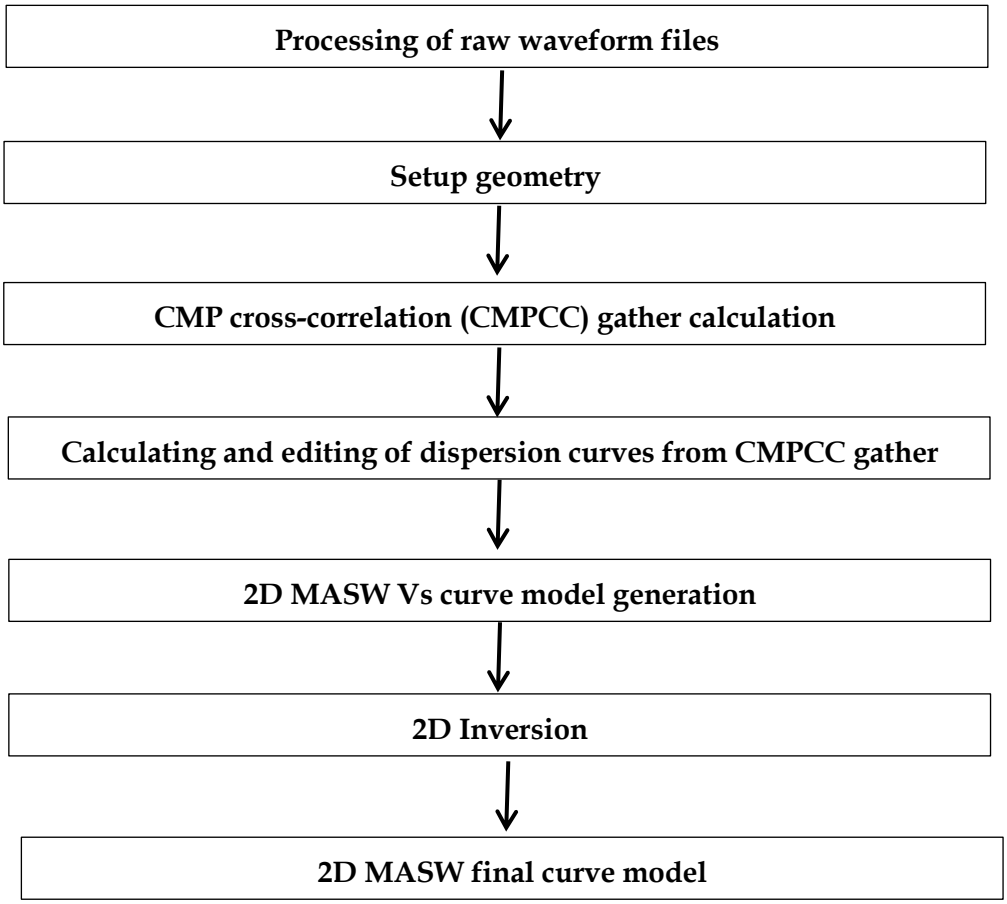

Figure 2: Flowchart depicting the processing steps.

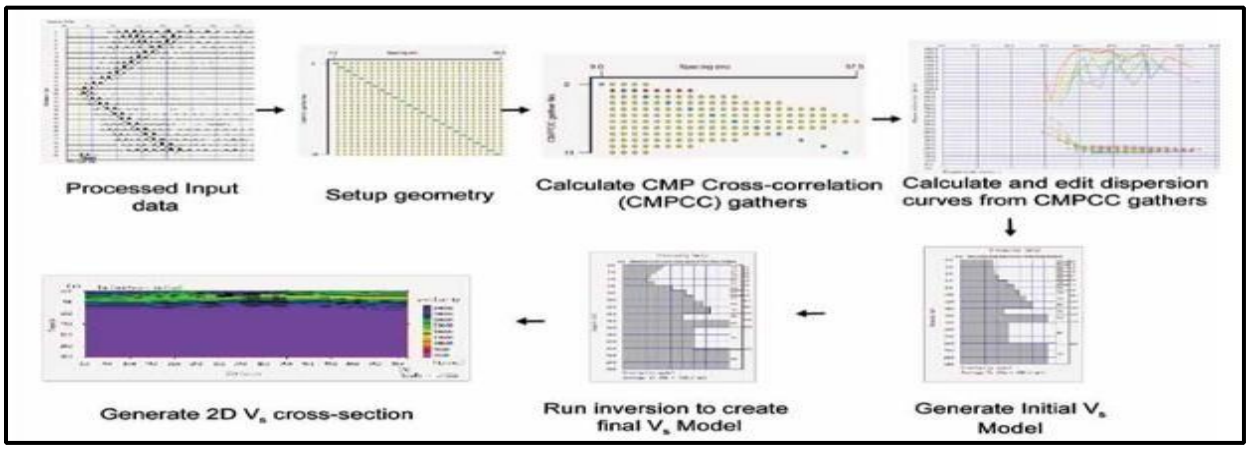

Figure 3: General processing steps used for MASW technique using the Seisimager/SW Software

The average upper 30m shear wave velocity was calculated from 2D horizontal averaged profiles by using equation (5)

$V_s\,30 = \frac{30}{\sum \frac{d}{V_s}}$ (Wair et al. 2012) …… (5)

The P- and S-wave velocities, as well as density values were computed using mathematical model (Table 3) to generate geotechnical parameters in other to have a better understanding of the subsurface rocks for building construction. The parameters generated were further used for classifying subsurface rocks and soils into different engineering competencies zones (Table 2).

The Poisson's ratio is a lithologic indicator and was estimated using equation (6).

$$\sigma = \frac{1}{2}\left[1 - \frac{1}{\left(\frac{V_s}{V_p}\right)^2 - 1}\right] \quad \ldots\ldots\ldots\ldots\ldots\ldots\ldots\ldots\ldots\ldots\ldots\ldots \quad (6)$$

The concentration index, known to be material dependent and usually revealing the material concentration or competence for foundation and other civil engineering purposes, was estimated using equation (7). This parameter is usually influenced by the elastic moduli of the material and the depth – pressure.

$C_i = \frac{1+\sigma}{\sigma}$ Bowles (1982) …… (7)

Abd El-Rahman (1991) defines C_i in terms of P- and S-wave velocities V_P and V_S as:

$$C_i = \left[3 - 4\left(\frac{V_s^2}{V_p^2}\right)\right] / \left[1 - 2\left(\frac{V_s^2}{V_p^2}\right)\right] \quad \ldots\ldots\ldots\ldots\ldots\ldots\ldots\ldots\ldots\ldots\ldots\ldots \quad (8)$$

The material index defines the material quality for foundation purposes. It is an indicator of the degree of competence of a material and is based on the elastic moduli (Abd El-Rahman, 1989). It is influenced by the material composition, degree of consolidation, fracturing, jointing, and presence or absence of fluid in pore spaces, thus, affecting the wave velocity. The material index is computed using equation (9).

$$M_i = 1 - 4\sigma = \frac{\mu - \lambda}{\mu + \lambda} \quad \ldots\ldots\ldots\ldots\ldots\ldots\ldots\ldots\ldots\ldots\ldots\ldots\ldots\ldots \quad (9)$$

Where μ and λ represent the rigidity and Lame's constant, respectively.

Finally, the stress ratio was computed (equation 10) to determine the consolidated settlement, an equilibrium steady-state condition of zero lateral and vertical strains (Bowles, 1982).

$$S_i = \frac{\sigma}{1 - \sigma} \quad \ldots\ldots\ldots\ldots\ldots\ldots\ldots\ldots\ldots\ldots\ldots\ldots\ldots\ldots \quad (10)$$

=

Table 2a: Estimation of Soil Dynamic Parameters (Concentration Index (Ci) and Stress Ratio (Si)) (Khalil and Hanafy, 2008)

Soil Description Parameter	WEAK		FAIR		GOOD
	Incompetent		Fairly Competent		Competent
	Very Soft	Soft	Fairly competent	Moderately competent	Compacted
Concentration Index (Ci)	3.5 - 4.0	4.0 - 4.5	4.5 - 5.0	5.0 - 5.5	5.5 - 6.0
Stress Ratio (Si)	0.7 – 0.61	0.61 – 0.52	0.52 – 0.43	0.43 – 0.34	0.34 – 0.25

Table 2b: Estimation of Soil Dynamic Parameters (Poisson's Ratio (σ) and Material Index (V) (Khalil and Hanafy, 2008)

Soil Description Parameter	Incompetent to Slightly competent	Fairly to Moderate competent	Competent materials	Very competent materials
Poisson's Ratio (∂)	0.41-0.49	0.35 – 0.27	0.25 – 0.16	0.12 – 0.03
Material Index (V)	(-0.5)- (-1)	(-0.5)- (0.0)	0.0 – 0.5	> 0.5

Table 3. List of equations used to calculate elastic moduli

Elastic Modulus	Used Equation	Reference
Shear Modulus	$\mu = \frac{E}{2(1+\sigma)}$	King (1966), Toksoz et al (1976)
Young's Modulus	$E = \rho\left[\frac{3V_p^2 - 4V_s^2}{(V_p/V_s)^2 - 1}\right]$	Adams (12)
Poisson's Ratio	$\sigma = \frac{1}{2}\left[1 - \frac{1}{(V_p/V_s)^2 - 1}\right]$	Adams (12), Salem (16)
Lame's Constants	$\lambda = \frac{\sigma E}{(1+\sigma)(1-2\sigma)}$	King (1966), Toksoz et al (1976)

V_p and V_s are the P- and S-wave velocities respectively

Result and Discussion

Multichannel Analysis of Surface Wave (MASW)

Table 4: Results of Multichannel Analysis of Surface Wave (MASW)

Traverses (TR)	Layers	Horizontal range (m)	Depth range (m)	Shear wave velocity $V_s(ms^{-1})$	Lithology
1	1	6-60, 6-42	1-4,6-19	290-390	Clayey sand
	2	35-60, 19-54	6.3-11.4, 19-24	423-525	Gravelly sand
	3	23-28	23-28	540-590	Firm soil
2	1	6-66	0-8	334-427	Clay/Stiff
	2	6-66	9-19	458-552	Sand/Gravelly
	3	6-66	20-27.5	583-615	Firm soil
3	1	36-88	0-4	396-520	Sand
	2	7-60	5-22, 8-15	396-570	Clayey sand
	3	0-52	23-27	568-571	Gravelly
4	1	2-27	2-4	92-162	Clay
	2	2-39	15-24	184-246	Silty Clay
	3	2-39	25-27	215-262	Stiff Clay/ Sand

5	1	11-60	0-4	238-288	Silty Clay
	2	4-43	5-12, 2.1- 14, 13-20	304-354	Sandy Clay (Silty clay)
	3	4-60	21-27	270-380	Sand
6	1	4-15, 84-99, 24-83	0-5, 0-6,10-14 8-12	346-520 259-433	Sandy soil/Sand
	2	80-99,	0-7,7-20	607-995	Clayey sand
	3	24-83, 4-99 4-99	15-27	868-1042	Gravelly Firm soil

The 2D shear waves velocity (Vs) models for the six traverses (TR1-TR6) obtained from the analysis of MASW field data are shown in Fig. 4(a – f). The velocity distribution is the physical parameter used in surface wave models. Visual inspection of inverted Vs models showed 3-4 distinct layers were mapped with general increase in Vs with depth, the Vs model revealed the heterogenous nature of the subsurface layers of the study area (Fig. 4a, 4b, and 4f). The depth of investigation obtained is in the range of 27 to 30m over a lateral spread ranging from 38 – 99 m. In some of Vs models, perturbation of the high-velocity layers by low-velocity layers is clearly observed. This could reflect the unstable nature due to low compactness of the soils beneath the investigated area. The velocity sections show that Vs varies from $97ms^{-1}$at the surface to $1024ms^{-1}$ in the deepest part of the profiles. The closeness of these inverted models in spite of the uncertainties arising from non-uniqueness of inversion models and the smearing effect that characterized the surface wave analysis underscores the choice of the integrated approach used in this study. The borehole data collected prior to the geophysical surveys provided the baseline for identification and delineation of the various strata. The table 4 showed the lateral range, depth range, shear wave velocity and lithology of six traverses. For the Vs models along TR 1, at horizontal distance 6-60 m, 6 – 42 m, with corresponding depths ranging from 1 – 4m, 6 – 19 m respectively and velocity values ranging from 290 -$390ms^{-1}$ is a representative of clay to sandy soil (Borchedt, 1994). At 35 – 60 m and 19 – 54 m lateral distance and 6.3 – 11.4 m, 19 – 24 m depth, the S-wave velocity ranges from 423 – $525ms^{-1}$ is an indicative of gravelly soil. The layer within the depth range 23 – 28 m consist of firm soils with S-wave velocity values ranging from 540 – $590ms^{-1}$ (Table 4). he gravelly soil and firm soil are suggestive of competent subsurface

materials which could support foundation of engineering structures. The lithology revealed under TR 2 are the clay/stiff soil with S-wave velocity ranges from 334 – 427 m/s and depth from 0 m - 8m. From depth of 9 – 19m is an indicative of sand/gravelly soils at lateral distance of 6 – 66 m and S-wave velocity values ranging from 458 – 552ms^{-1}. Across the profile at depth of 20 – 27.5 m and S – wave velocity values of 583 – 615ms^{-1} is an indicative of firm soils (Borcherdt, 1994) (Table 4). The firm soil at the base is suggestive of competent subsurface materials which could be suitable for supporting foundation of engineering structures. Along TR 3, From the surface to depth of 4m and lateral distance of 36 – 88 m is a representative of clay/stiff clay with S-wave velocity values ranges from 174 – 307ms^{-1}. From depth of 5 – 22m across the profile, the S-wave velocity ranges from 396 – 520ms^{-1} indicating sand while in between this section lies the clayey sand which exist from depth of 8 – 15 m at lateral distance of 7 – 60m. Beneath this section lies the gravelly soil which extends to the depth of 27 m with shear wave velocity (Vs) ranging from 568 – 571ms^{-1} (Table 4). The clayey materials within this location could be responsible for the sinking of building**.** Under TR 4 are three distinct layers namely clay, silty clay and stiff clay/sandy soil. The S- wave velocity across this zone ranges from 97 – 307ms^{-1}. At depth of range between 2 - 14 m and horizontal distance of 2- 27 m is suggestive of clay with s- wave velocity of 97 - 162ms^{-1}. Beneath this layer exist silty clay which extends to depth of 24 m across the entire profile with S-wave velocity of range 184 – 240ms^{-1}. From depth of range 24 – 27 m across the entire profile is symptomatic of stiff clay/sandy soil with S – wave velocity of 215 – 262ms^{-1}. These clayey layers are inimical to foundation of engineering structures.

The lithology under TR 5 showed three layers to a depth of about 27 m. The first layer is an indicative of silty clay with S-velocity values ranging from 238 – 288ms^{-1} to a depth range of 4 m, beneath this is sandy clay (Vs ranging between 304 – 354ms^{-1}) at lateral distances; 4 -43, 460 m and corresponding depths; 5-12m, 13 – 20m. This was sandwich with silty clay which exist from depth of 2.1 – 14 m at lateral distance of 11 – 60m. Beneath this section lies sand layer which extends to a depth of 27 m with S-wave velocity of range 270 – 380ms^{-1}. TR 6 is characterized with materials with Vs that spans between 346 – 520ms^{-1} along the lateral distances; 4- 15 m, 26 -60 m, 83 – 90 m at corresponding depths; 1 - 5 m, 11 -15m, and 1- 6 m, this material is

representative sandy soils/sand (Borcherdt, 1994) and this corroborate the result of the Inverted resistivity model. At lateral distances of 4 – 49 m and depth of 15 – 27m, the S-wave velocity (Vs) of range of 868 – 1042ms^{-1} connate firm soil. The inferred near surface geological material are suspected to be incompetent to support engineering foundation. Only the gravelly and firm soils at depth of 15-27m are competent to support heavy engineering foundation. The range of Vs obtained for the three geological units mapped in this study agrees well with the earlier works (Oyedele and Olorode, 2010).

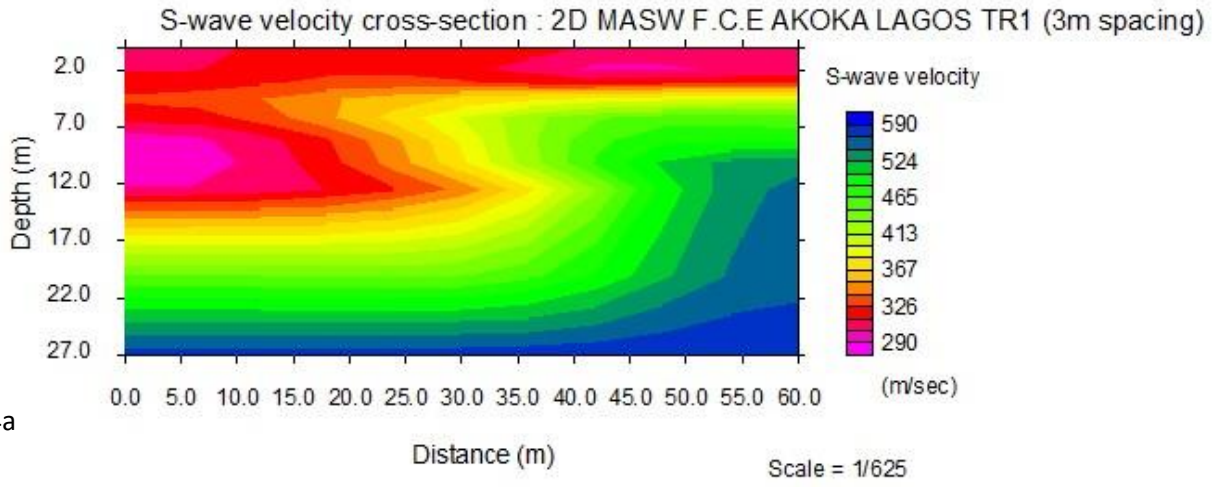

4a

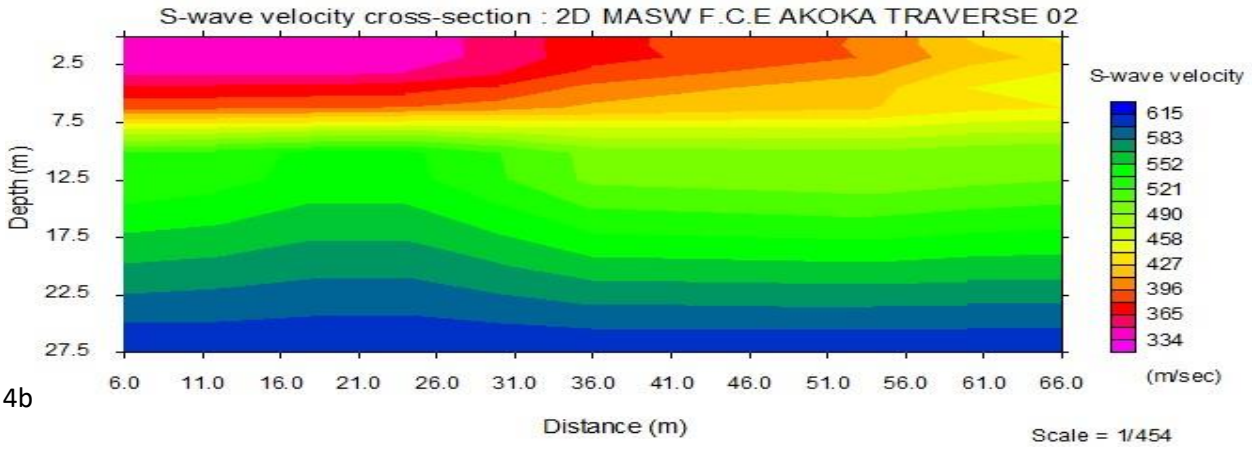

4b

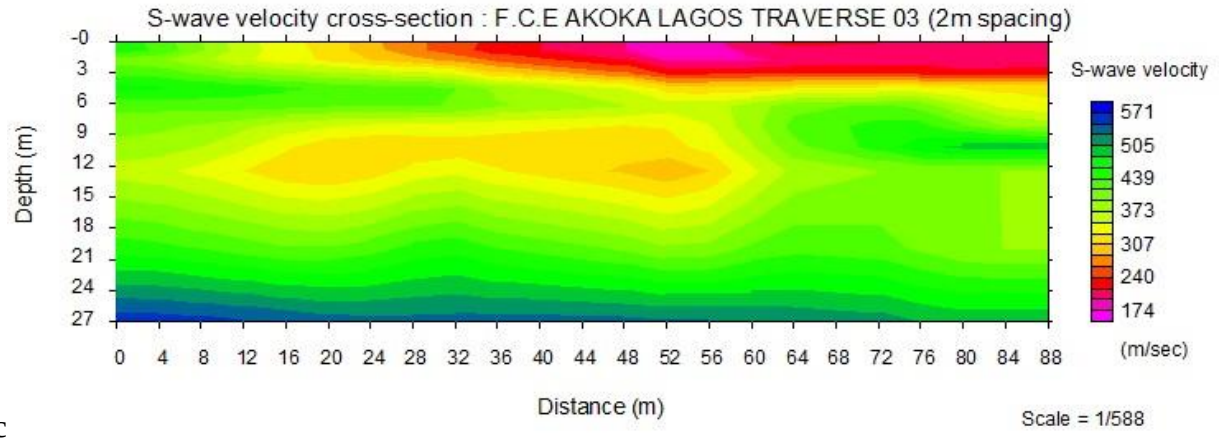
S-wave velocity cross-section : F.C.E AKOKA LAGOS TRAVERSE 03 (2m spacing)
Depth (m)
-0
3
6
9
12
15
18
21
24
27
0 4 8 12 16 20 24 28 32 36 40 44 48 52 56 60 64 68 72 76 80 84 88
Distance (m)
S-wave velocity
571
505
439
373
307
240
174
(m/sec)
Scale = 1/588

4c

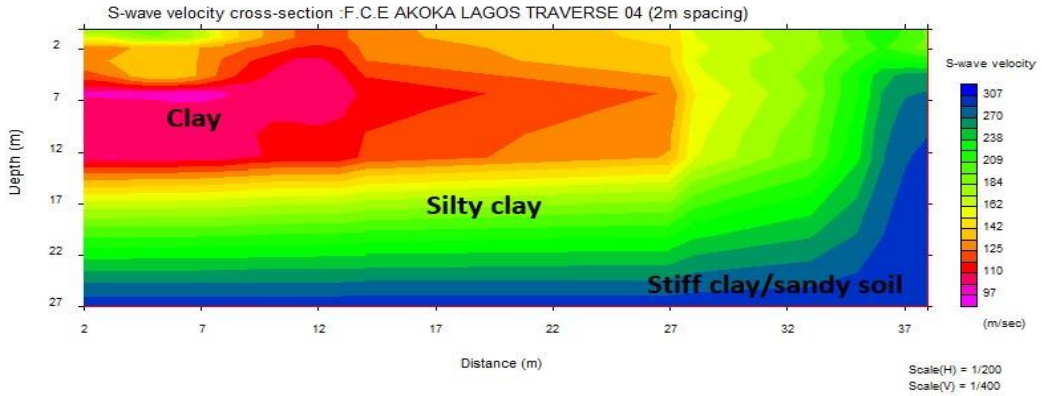
S-wave velocity cross-section :F.C.E AKOKA LAGOS TRAVERSE 04 (2m spacing)
Depth (m)
2
7
12
17
22
27
Clay
Silty clay
Stiff clay/sandy soil
2 7 12 17 22 27 32 37
Distance (m)
S-wave velocity
307
270
238
209
184
162
142
125
110
97
(m/sec)
Scale(H) = 1/200
Scale(V) = 1/400

4d

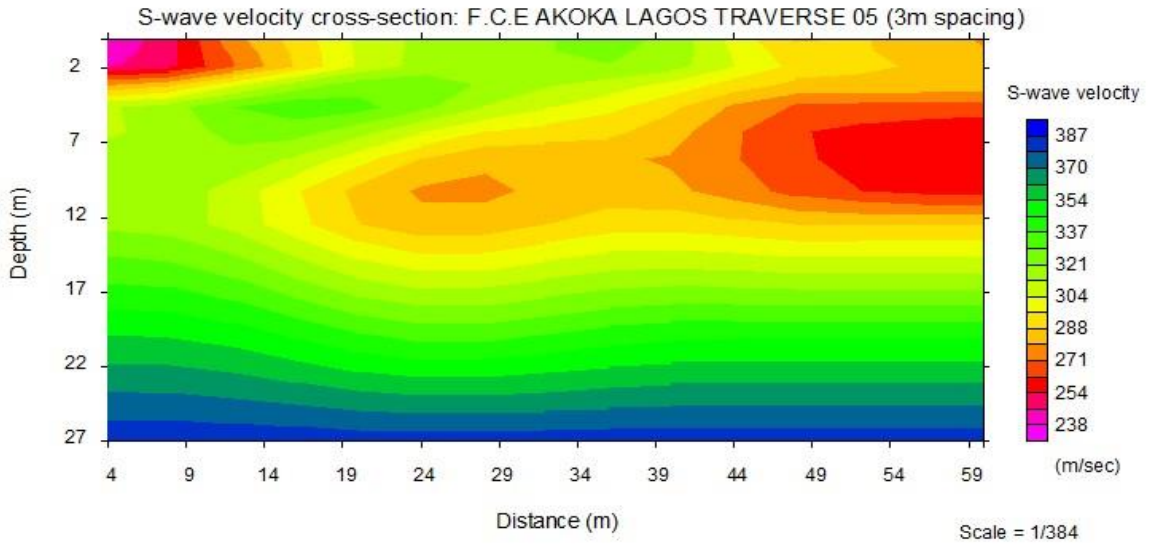
S-wave velocity cross-section: F.C.E AKOKA LAGOS TRAVERSE 05 (3m spacing)
Depth (m)
2
7
12
17
22
27
4 9 14 19 24 29 34 39 44 49 54 59
Distance (m)
S-wave velocity
387
370
354
337
321
304
288
271
254
238
(m/sec)
Scale = 1/384

4e

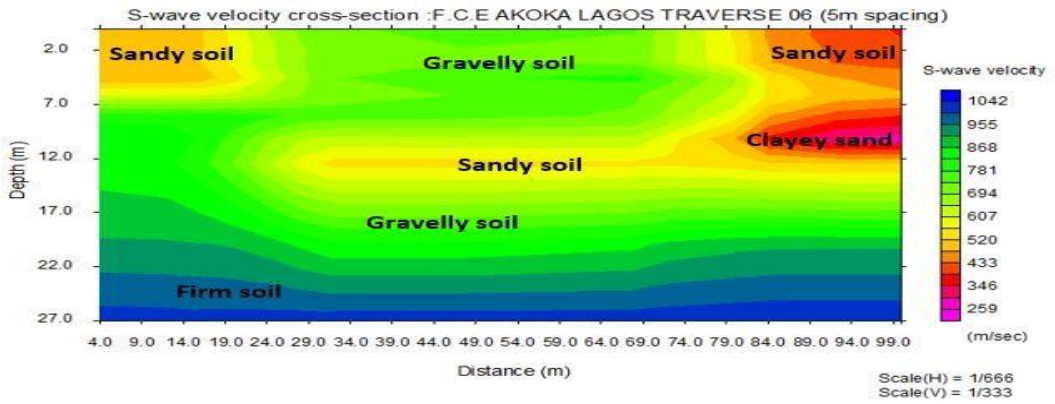

4f

Figure 4(a – f): Seismic velocity model along TR1 – TR6.

Engineering Parameters

No construction material has more variable engineering and physical parameters than the ground's soil. These parameters vary both horizontally and vertically and often the variations are strong (Bowles, 1982). In order to evaluate the competence of the subsurface for construction, some of the shallow engineering parameters were calculated. Three parameters were calculated; the Concentration Index (Ci), the Material Index (V) and the Stress Ratio (Si). Integration of these three parameters was used to select the most appropriate layer for construction. To calculate engineering parameters given in Table 2a and 2b, the values of P-wave velocity and S-wave velocity, Field density (ρ), Poisson's Ratio (σ), Young's Modulus (E), and the Shear Modulus (μ) were required. The calculated geotechnical parameter from all six profiles revealed three (3) geologic layers within the depth of investigation. Layer 1 whose depth ranges from 0 - 6.3 m have P-wave velocity ranging from 1414 m/s to 1780ms^{-1} and S-wave velocity ranging from 112ms^{-1}s to 442ms^{-1}. The poisons Ratio (σ) across the six profiles ranges from 0.46 - 0.49. It has a high Poisson ratio value thus, indicates that this layer is a slightly competent (Salem, 1990). The Young's modulus values ranging from 657 kpa to 1060 kpa. this range of value indicates a zone which is characterized by relatively low values of Young's Modulus. Also, the shear Modulus (μ)/Rigidity values (22 kPa to 365 kPa) indicated a low rigidity zone., the concentration index

(Ci) (3.01 - 3.14), material index (ν) (−0.9 to -0.86), stress ratio (Si) (0.88 to 0.99) values are reflection of weak incompetent soil (very soft soil).

Layer 2 across the six profiles have depth range of 3.1 m to 20 m with P-wave and S-wave velocity ranging from 1411ms^{-1} to 1774ms^{-1} and 109ms^{-1} to 436ms^{-1} respectively. The poisons Ratio (σ) (range from 0.46 - 0.49), Young's modulus (ranges from 61 kPa to 1043 kPa), Shear Modulus (μ)/Rigidity (ranges from 20 kPa to 357 kPa) across the six profiles are indication of incompetent to slightly competent zone (Salem, 1990). The calculated values of concentration index (Ci) (3.01 - 3.13), material index (ν) (−0.98 to -0.87) and Stress Ratio (Si) (ranges from 0.88 to 0.99) across the second layer reveals an incompetent soil layer.

Third layer falls within a depth range of 12.5 – 30 m across the six traverses.

The P-wave and S-wave velocity values ranges from 1630 m/s to 2144 m/s and 306 m/s to 769 m/s respectively. The Poison's Ratio (σ) (values ranges from 0.42 - 0.48), Young's modulus (values ranges from 504 kPa to 332534 kPa), Shear Modulus (μ)/Rigidity (ranges from 170 – 117089 kPa) is an indication of incompetent to slightly competent zone (Salem, 1990). The calculated concentration index (Ci) reveals values of 3.07 – 3.34. This indicates that the area is characterized by relatively low concentration index reflecting weak incompetent soil (very soft to soft soil). The calculated material index (ν) for third layer revealed value of −0.92 to -0.70 across all profiles. The area is characterized by relatively low Material Index (ν) which reflects incompetent soil to competent. The calculated Stress Ratio (Si) varies from 0.74 to 0.93. This indicates that layer 3 of the study area is characterized by low Stress Ratio (Si) thus, reflecting an incompetent soil layer.

Conclusion

Three subsurface layers were delineated from MASW, the first layer is characterized by relatively low concentration index (Ci) values, which reflects weak incompetent soil (very soft to soft soil). The material index (ν) ranges from −0.9 to -0.86 across all profiles, reflecting weak incompetent soil (soft). The Stress Ratio (Si) varies from 0.88 to 0.99 across the profiles. At the middle layers, the P-wave and S-wave velocity ranges from 1411 m/s to 1774ms^{-1} and 109ms^{-1} to 436ms^{-1}

respectively within the depth range of 3.1 m to 20 m. The poisons Ratio and Young's modulus values range from 0.46 to 0.49, and 61 kPa to 1043 kPa; shear modulus (μ)/Rigidity ranges from 20 kPa to 357 kPa, indicating an incompetent to slightly competent zone. The concentration index (Ci) (3.01 - 3.13) values across the second layer indicate that the area is characterized by relatively low concentration index (Ci) values reflecting weak incompetent soil (very soft to soft soil). The calculated material index (ν) (−0.98 to -0.87) reflected weak incompetent soil (soft). The Stress Ratio (Si) (0.88 to 0.99) also reflected an incompetent soil layer. Third layer have depths range 12.5 – 30 m, the P-wave and S-wave velocity ranging from $1630ms^{-1}$ to $2144ms^{-1}$ and $306ms^{-1}$ to $769ms^{-1}$ respectively. The poisons Ratio (σ) (0.42 - 0.48), Young's modulus (504 kpa to 332534 kpa), Stress Ratio (Si) (0.74 to 0.93) values reflected incompetent to competent soils.

The result of MASW along traverse 3 indicated incompetent clay/stiff clay zone at the surface to a depth of about 6m at horizontal distance 36 m – 88 m (fig 4c). These clayey materials could be attributed to the sinking of the building (fig 4c). It also revealed competent sand and gravelly sand layers between 18 m -21 m and 22 m – 27 m, respectively. The MASW result along traverse 4 (fig. 4d) revealed three incompetent zones of clay, silty clay, and stiff clay/sandy soils at depth range of 2 m -14 m, 15 m – 24 m and 24 - 27 m on lateral distances od 2 m - 7m, 2 m – 35 m and 2 m – 37 m respectively across the profile (Table 4). These three geological layers mapped are in agreement with the earlier works (Ajayi et al., 2023; Oyedele & Olorode, 2010).

These incompetent materials could also be attributed to the distressed and failed parts of the buildings in the study area. In this situation, shallow foundations might not be feasible in the affected locations, which were adopted because the incompetent subsurface materials are laterally and vertically extensive.

Recommendations

The following recommendations were made:

1. Use wider geophone spacing for deeper probe but smaller spacing for shallow probes
2. Ensure the use of multiple shots at near offsets which give high frequency/shallow data and far offsets for low frequency/ deep data.

3. The incompetent/slightly competent subsurface dominate the study area and should be properly dealt with before erecting a heavy structure on it.

References

Ajayi, A.A., Bakre, O.F., & Babatunde, P. (2023). Groundwater exploration of Federal College of Education (Technical), Akoka, Lagos, Nigeria Community using Schlumberger array. *International Journal of Scientific and Engineering Research, 14(3), pp. 1-10.*

Borcherdt, R.D. (1994). Estimation of site-dependence response spectra for design methodology and applications. *Earth Spectra*, 10(4), 617-653.

Bowels, J.E. (1984). Physical and geotechnical properties of soils. McGraw-Hill, London

El-Rahaman, A. (1989). Correlations between shear wave velocity and geotechnical parameters of Egyptian soils. Proceedings of 2nd International Conference on Soil Dynamics and Earthquake Engineering, Cairo, pp. 45- 52.

Ezersky, M., Leger, J.M., Djoe, K., & Akkawi, E. (2013). Integrated Geophysical Survey for delineation of subsidence-related deformation in the Dead Sea coastal area. *Journal of Applied Geophysics 93, 1-12*

Foti, S., Sambuelli, L., Valentina, L.S., Strobbia, C. (2003). Experiments of joint acquisition of seismic refraction and surface wave data. *Near Surface Geophysics*. (3):119–129. doi:10.3997/1873-0604.2003002

Hill, M.B., & Webb, J.E. (1958). The topography and physical features of Lagos harbour. *Phil Trans R Soc* (Series B). 241:319–333.

Jones, H.A., Hockey, R.D. (1964). The Geology of Part of Southwestern Nigeria. Geological Survey of Nigeria Bulletin, 31,87P.

Kearey, P., Brooks, M., & Hill, I. (2002). An Introduction to Geophysical Exploration. London: Blackwell Science Ltd. Kemna, A. 2000. Tomographic Inversion of Complex Resistivity: Theory and Application.

Khalil, A., & Hanafy, S.M. (2008). Estimation of Shear wave velocity and soil dynamics parameters using MASW. *Journal of Geophysics and Engineering, 5(2), 141-150.*

Lai, C.G., & Wilmanski, K. (2005). Surface waves in geomechanics: direct and inverse modeling for soils and rocks. Udine (Italy): International Centre for Mechanical Sciences. CISM Courses and Lectures. 481.

Le Ngal, N., Pramumijoyo, S., Satyarno, I., Brotopuspito, K.S., Kiyono, J., & Hartantyo, E. (2019). Multi-channel analysis of surface wave method for geotechnical site characterization in Yogyakarta, Indonesia. In *E3S Web of Conferences* EDP Sciences. 7:03006.

Omatsola, M.E., & Adegoke O.S., (1981). Tectonic Evaluation and cretaceous stratigraphy of the Dahomey Basin. *Journal of Mining Geology. 5(2): 78-83.*

O'Neill, A., (2003). Full-waveform reflectivity for modeling, inversion and appraisal of seismic surface waves dispersion in shallow site investigations. Ph.D Thesis. Geophysics.

Oyodele, K.F (2008). Effectiveness of the Electrical Resistivity Methods in Coastal Hydro geophysical studies. *Journal of Environmental Hydrology. 16 (16).*

Park, C.B, Miller, R.D., & Xia J. (1999). Multichannel analysis of surface waves. Geophysics. 64(3):800–808. doi:10.1190/ 1.1444590

Prudhomme, K.D., Khalil, M.A., Shaw, G.D., Speece, M.A., Zodrow, K.R., & Malloy, T.M. 2019. Integrated geophysical methods to characterize urban subsidence in Butte, Montana, USA. *Journal of Applied Geophysics*, *164*, 87-105.

Pugh, J.C. (1954). A classification of the Nigerian Coastaline. *Journal of W African Sci. 1:3–12.*

Rix, G.J., & Leipski, E.A., (1991). Spectral analysis of surface waves. Proceedings, 4th International Conference on Soil Dynamics and Earthquake Engineering, Mexico City, Vol 2, pp. 691-702.

Taipodia, K., Dey, A., & Sitharam, T.G. (2015). Site characterization using MASW and its correlation with geotechnical parameters. Proceedings of the 50th Indian Geotechnical Conference, Pune, India, pp.1-6.

Xia J, Miller RD, Park CB, Hunter JA, Harris JB, Ivanov J. (2002). Comparing shear-wave velocity profiles inverted from multichannel surface wave with borehole measurements. Soil Dynamics and Earthquake Engineering. 22(3):181–190. doi:10.1016/S0267-7261(02) 00008-8